Optics & Laser Technology 169 (2024) 110123

Contents lists available at ScienceDirect

Optics and Laser Technology

journal homepage: www.elsevier.com/locate/optlastec

Full length article

Laser cladding of stainless-steel ball valves by a high-power diode laser source with a rectangular beam spot

Hongbo Zhu [a], Xingchen Lin [a], Xulan Xue [a], Yawei Zhang [a], Lijun Wang [a], Yongqiang Ning [a], Yijia Dong [a,b,*], Xuan Fang [c,*]

[a] State Key Laboratory of Luminescence and Applications, Changchun Institute of Optics, Fine Mechanics and Physics, Chinese Academy of Sciences, Changchun 130033, China

[b] University of Chinese Academy of Sciences, Beijing 100049, China

[c] State Key Laboratory of High Power Semiconductor Lasers, School of Physics, Changchun University of Science and Technology, Changchun 130022, China

ARTICLE INFO

Keywords:
Diode laser
Laser cladding
High power
Stainless-steel material
Ball valve

ABSTRACT

In this paper, the laser cladding of Ni60 + WC powder on the stainless-steel ball valves is investigated to improve the corrosion resistance and the wear resistance of industrial ball valves. A 2-kW high-power diode laser source based on beam multiplexing is used as the processing source to clad the ball valves. To make this diode laser source more reliable for laser cladding, a homogenizing optical system is designed and optimized to transform a circular beam spot output from the optical fiber to a rectangular spot with a flat-top distribution. Employing this diode laser source, the laser cladding of the stainless-steel ball valve is successfully achieved by use of the pre-set powder feeding. The hardness testing experiments are then performed on the ball valves of different diameters, followed by the evaluation of the thickness and hardness of the cladding coating. It is experimentally demonstrated that the microhardness of the ball valves is improved by 2.7 times and the cladding layer has no cracks, which proves the superior performance of the stainless-steel ball valves by use of the proposed method.

1. Introduction

Laser cladding as an advanced technology has been widely applied in many industrial fields to repair metallic components subjected to severe operating conditions. It can melt the cladding material and the metallic surface to form a cladding coating, which dramatically improves the corrosion resistance and the wear resistance of the metallic components [1,2]. In contrast to conventional material surface modification methods, laser cladding has been received greater acceptance by industry due to the unique advantages, such as low dilution, good metallurgical bonding, and fine grain size [3–7]. Among the various types of laser sources for laser cladding [8–11], the recently developed high power direct diode lasers (HPDDL) is characterized by high electro-optical efficiency, high reliability and low maintenance cost. Moreover, the metallic material presents a higher absorption for HPDDL than other laser sources because of the shorter wavelength of HPDDL. All these merits make HPDDL stand out for laser cladding that requires high cladding speed and high processing efficiency. Therefore, over the past several years, the laser cladding based on HPDDL have broadly attracted attentions of many research communities. Y Ding et al. used a 2-kW HPDDL to clad Stellite alloy mixture on the seat surface of a control valve, aiming at enhancing the hardness and the wear resistance [12]. Z Zhang et al. employed an 8-kW HPDDL to clad the 420 stainless steel power with 4 % molybdenum on the A36 mild steel plates, in order to increase the corrosion resistance of mild steel materials [13].

Although there are plenty of scientific research containing information about laser cladding by HPDDL [14–16], detailed investigations on the laser cladding of stainless-steel ball valves are rarely reported in the literature. It is well-known that stainless-steel ball valves are typically used as important components in the petrochemical industry [17]. The surfaces of ball valves are critical for reliable sealing operation; thus, they must be capable of withstanding very high contact stress without cracking, severe wear, and corrosion. Nevertheless, the pitting and spalling easily occur on the surface of ball valves after they operate for a long time, which seriously affects the leak proofness. This phenomenon can be attributed to the low hardness and poor wear resistance of stainless-steel material, which makes these ball valves cannot subject to the severe operating conditions for a long time. Therefore, the diode

* Corresponding authors.
E-mail addresses: dongyijia20@mails.ucas.ac.cn (Y. Dong), fangx@cust.edu.cn (X. Fang).

https://doi.org/10.1016/j.optlastec.2023.110123
Received 20 March 2023; Received in revised form 2 August 2023; Accepted 25 September 2023
Available online 1 October 2023

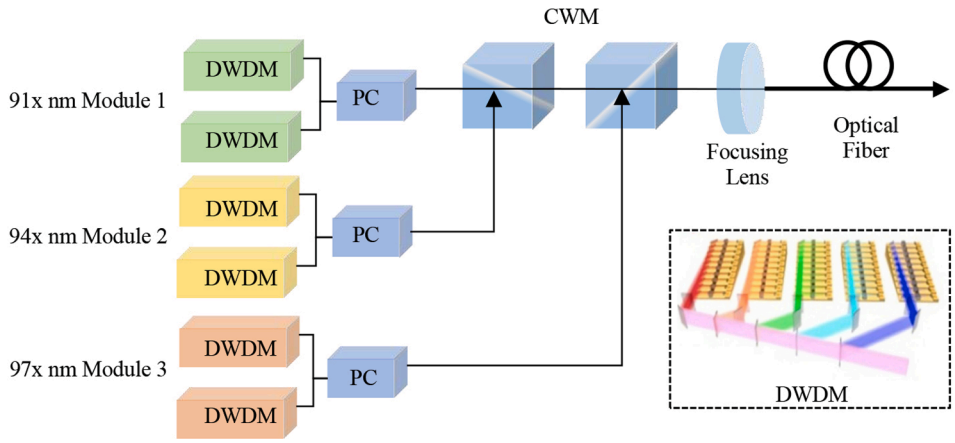

Fig. 1. Schematic of the optical structure of diode laser source. DWDM: dense wavelength division multiplexing; PC: polarization combining; CWM: coarse wavelength multiplexed.

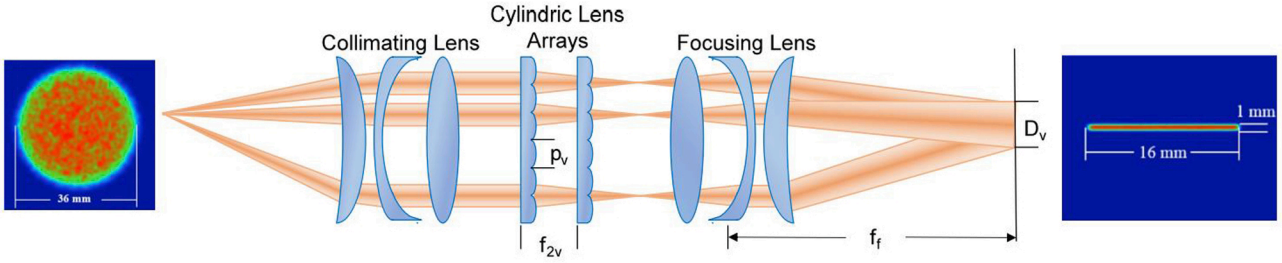

Fig. 2. Schematic of HOS and light intensity distribution diagram before and after the light spot passes through the HOS.

Table 1
Chemical composition of Ni60 powder.

	Chemical composition (%)					Fineness
	C	Cr	Si	Fe	Ni	
Ni60	0.78	15.9	4.55	5.0max	Bal	150/300#
WC	Purity > 99					140/300#

laser cladding is necessary, and the investigation of processing experiment and cladded samples measurement can provide a theoretical guidance on the surface modification of stainless-steel ball valves. A stack array is used as a unit device in the traditional diode laser cladding light source for beam combination. A rectangular spot can be formed directly after beam focusing, which can achieve the large area cladding. However, the lifetime of this diode laser is short due to the poor heat dissipation performance [18]. The output spot of the new generation of fiber-coupled diode laser source is a point spot with a diameter of 2 mm. The cladding speed is required to be slow and processing requirement at the overlap is high, otherwise defects will occur [19]. Therefore, a large-area, high-efficiency and defect-free processing method using diode lasers is needed [20].

The goal of this paper is to investigate the performance of the laser cladding of Ni60 + WC powder on the stainless-steel (3 0 4) ball valves. A 2-kW HPDDL based on beam combination is employed for the experiment. Using a set of homogenization optical system (HOS), the energy distribution of output beam from the optical fiber is converted from a Gaussian-like distribution to a flat-top distribution, which makes this diode laser source more reliable in the laser hardening. Employing this diode laser source, laser cladding experiments are performed on the ball valves of different diameters. The thickness and hardness of cladding coating are evaluated. By optimizing processing parameters of the laser hardening, a maximum Rockwell hardness of 647$HV_{0.1}$ and a uniform cladding thickness of 1.4 mm are obtained on the ball valves. No visible crack is found in the cladding coating of the stainless-steel ball valve, which proves this processing method can decrease the cracking sensitivity and eliminate defects effectively.

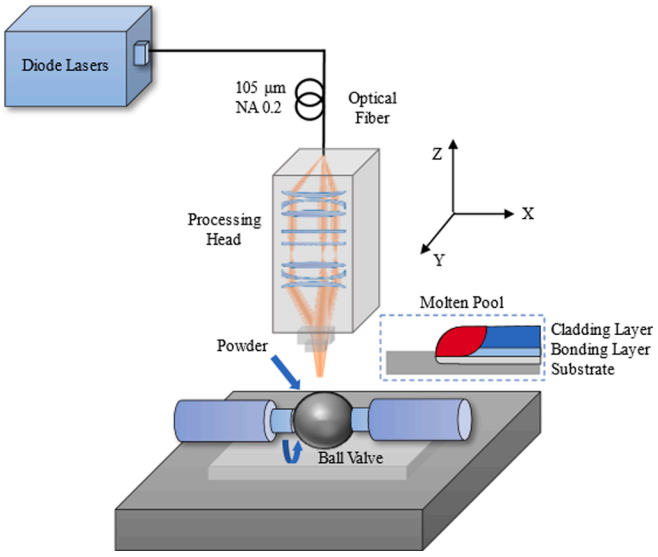

Fig. 3. Schematic of the whole laser processing setup.

2. Design of experiments

2.1. Specifications of diode laser source

In this work, the key component for the laser cladding is a 2-kW high power direct diode laser. The unit devices in this diode laser source are commercially available building blocks that are manufactured based on

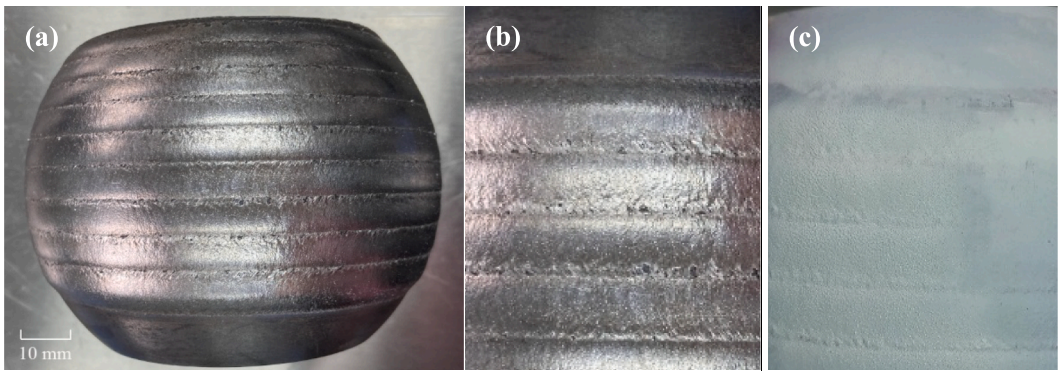

Fig. 4. Liquid dye penetrant test with color indication for cracks inspection. Surface photographs of (a) cladded ball valve, (b) before and (c) after test. No cracks are found in the cladding layers.

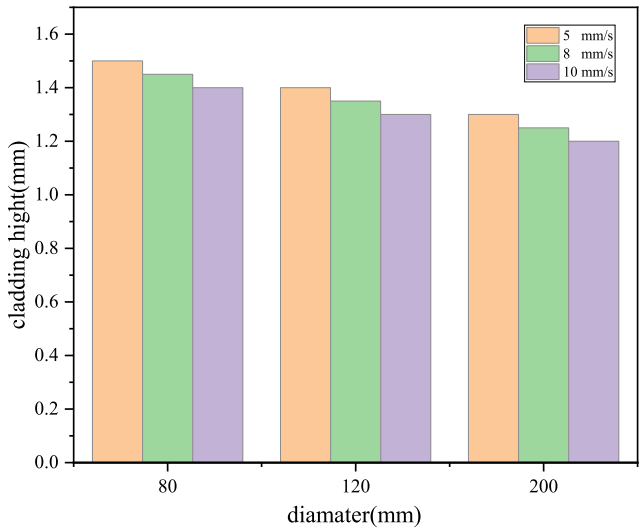

Fig. 5. Cladding height measurement for ball valves with different diameters for different processing speeds (shown in different colors).

the technology platform of single diode laser emitter multiplexing. Firstly, the output laser beams from five building blocks are dense wavelength division multiplexing (DWDM) using reflective volume Bragg gratings (VBGs). Subsequently, after DWDM, the multiplexed laser beam experiences polarization multiplexing to double its power and brightness at a constant beam quality. Similar results are obtained in turn with three diode laser multiplexed modules that lased at 91x nm, 94x nm, and 97x nm, respectively. Finally, these three wavelength channels are coarse wavelength multiplexing (CWM) using dielectric filters. The internal optical structure of the diode laser source has been previously introduced in [21], so we briefly describe it here. The output beam after coarse wavelength multiplexing is coupled into the commercially available quartz block high-power (QBH) fiber with the core diameter of 105 μm and the numerical aperture of 0.2. Because the diode laser source is manufactured by multi-wavelength multiplexing, the output wavelength is a multiplexing of 91x nm, 94x nm and 97x nm. At a coolant temperature of 25 °C and in a continuous wave (CW) operating mode, the diode laser source can produce 2045 W power from the optical fiber at an injection current of 10 A. The schematic of the complete diode laser source is shown in Fig. 1.

In the laser cladding, it is necessary to make multiple passes on the metallic surface if the size of the laser focal beam is not long enough to cover the entire processing area. Thus, a sufficiently long focal beam with the flat-top distribution is needed to improve the processing quality, increase the processing efficiency, and reduce the impact of the temperature gradient. Nevertheless, the commercial fiber coupled diode laser usually yields a circular laser beam with a Gaussian-like distribution, leading to a small focal beam spot with the diameter of 100–1000 μm. Thus, a set of HOS is designed and installed at the end of the optical fiber for converting the focal beam from a Gaussian-like distribution to a flat-top distribution. As shown in the schematic of structure in Fig. 2, the HOS is composed of collimating lens group, cylindrical lens arrays (CLAs), and focusing lens group.

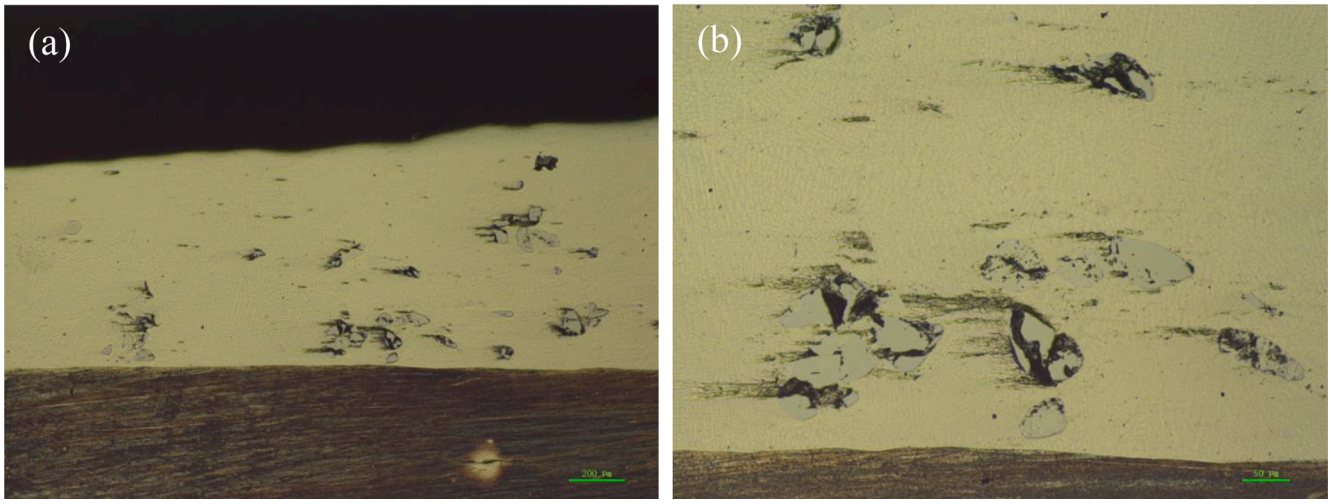

Fig. 6. Cross-sectional micrographs of the cladded specimen under (a) 50× magnification and (b) 200× magnification.

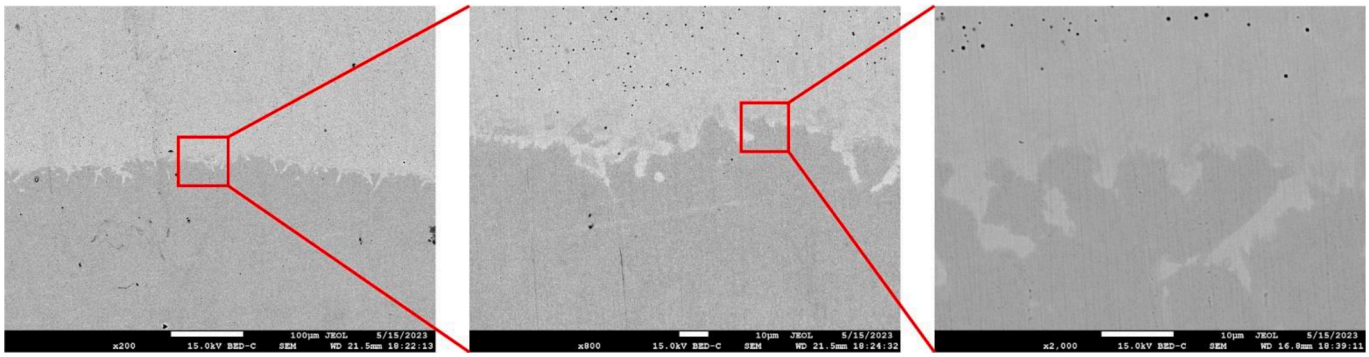

Fig. 7. SEM images of the interface between the cladding layer and substrate. Regions of interest are magnified from left to right.

The collimating lens group is a set of triplet lenses with a focal length of 100 mm, and the spherical aberration of the beam can be eliminated by the triplet lenses. The principle of homogenization is that the CLAs split the wave front of the collimated laser beam into many small ones, which are then focused and overlapped by the field mirrors. Since CLAs split the incident laser beam in only one direction, the focal beam is flat-topped in one direction while the beam in the other direction remains well focused into a Gaussian-like distribution. The focal length of focusing lens group is 350 mm. The size of the focal beam is calculated by

$$D_v = p_v \times \left(\frac{f_f}{f_{2v}}\right), \tag{1}$$

where p_v, f_{2v}, f_f respectively denotes the pitch, the focal length of the second CLA, and the focal length of the field lens. D_v denotes the size of the focal beam. From Eq. (1) we can see that the imaging characteristics of HOS are mainly regulated by the radius of the lens surface and the pitch of cylindrical lenses. In consideration of the homogeneity and the beam size in the actual processing, the pitch and radius are set to be 0.5 mm and 16 mm, respectively. As a result, a linear focal beam spot with an effective size of approximate 16 × 1 mm^2 is obtained at the focal plane. It is worth noting that the beam is focused to a homogeneous linear shape spot along one direction, and meanwhile it is tightly focused along the other direction. This uniform energy distribution of the focused beam spot provides a smooth heating and cooling cycle during the cladding process, which can effectively increase the processing speed and reduce the thermal stress of the processed samples.

2.2. Materials

The metallic part for the laser cladding is the ball valve that is usually employed in the transportation of petroleum and chemical liquids. The material of the ball valve is 304 stainless-steel (304SS), and the hardness of the ball valve is about 210 $HV_{0.1}$. In the petrochemical industry, the common diameters of ball valves are from 100 mm to 2000 mm. However, as the ball valve size decreases, the contractility will increase, which becomes more challenging to eliminate cracks after the laser cladding process. Therefore, three ball valves with relatively small diameters of 80 mm, 120 mm, and 200 mm are adopted in the experiment to evaluate the cladding effect.

The Ni-based alloy powder is extensively used in the laser cladding because of the characters of the corrosion resistance and the wear resistance. In the experiment, the Ni-based alloy powder added with hard ceramic particles tungsten carbide (Wt. ratio: 100:30) is selected as the cladding powder. The chemical composition of Ni60 + WC powder is shown in Table 1. The size of the Ni60 powder particle is in the range of 80–100 μm and that of the WC powder particle (angular shape) is in the range of 45–100 μm.

2.3. Experimental setup

In the experiment, the laser cladding is carried out using an industrial processing system, consisting of a 6-axis robotic arm and a computer numerical control (CNC) table. The diode laser source is integrated into this industrial system. Both the laser processing head and the powder feeding nozzle are fixed on the 6-axis robotic arm. Besides, the CNC table is employed to carry the ball valve and rotate it with respect to the laser processing head. The schematic of the whole laser processing setup is shown in Fig. 3. The laser beam is vertical to the ball valve surface. During the processing, the surface of the ball valve is adjusted to the focal plane of the laser processing head, and the working distance is kept constant for all the experiments. An off-axial auto feeding powder equipment is utilized as the powder feeder, and the lateral nozzle is set at a 45° angle from the horizontal direction. By means of the pre-placed powder feeding, the cladding powder is deposited on the ball valve and before the focal beam spot. The thickness of pre-placed powder was approximately 2.5 mm. With the rotation of the ball valve, the cladding powder is delivered into the molten pool, and then rapidly melted and solidified to the cladding layer. The rectangular exit of the feeding nozzle with a dimension of 10 mm × 2 mm is to match the shape of the focal spot. High purity nitrogen gas with a flow rate of 15 L/min is applied as a shielding gas to shield the molten pool from oxidation.

3. Results and analysis

As mentioned previously, three ball valves with diameters of 80 mm, 120 mm, and 200 mm are laser cladded at different processing speeds (i.e., 5 mm/s, 8 mm/s, and 10 mm/s). An overlap ratio of 50 % is adopted for the multi-track laser cladding in the processing, which can produce a uniform thickness of the cladding layer. Firstly, the macroscopic morphology of the ball valves is observed. The cladded ball valves exhibit a smooth and regular shape, which indicates that the diode laser source can yield a rectangular beam focal spot with a stable and uniform energy distribution. The melting of the base material produces a dilution of the clad powder; therefore, the composition of the coating is an alloy formed by 304SS and Ni-based powder. Then, a liquid dye penetration test is used to detect the cracks in the cladding coating. In this way, the cladding ball valves can be visually inspected. As shown in Fig. 4, no cracks are found in the cladding layer, preliminarily demonstrating that the proposed method can effectively eliminate cracks.

It is necessary to determine the relationship between scanning speed and coating thickness. Thus, samples are cut from cladded ball valves using a wire-electrode cutting machine for microstructure analysis. The nine samples are processed and labelled as sample1 to 9. The thickness of the coating is examined by use of optical microscopy, as shown in Fig. 5. On one hand, for the ball valves with the same diameter, the cladding height represents a declining trend with the increasing scanning speed. This can be explained that the faster processing speed leads to relatively fewer laser energy radiated on the local area of the ball

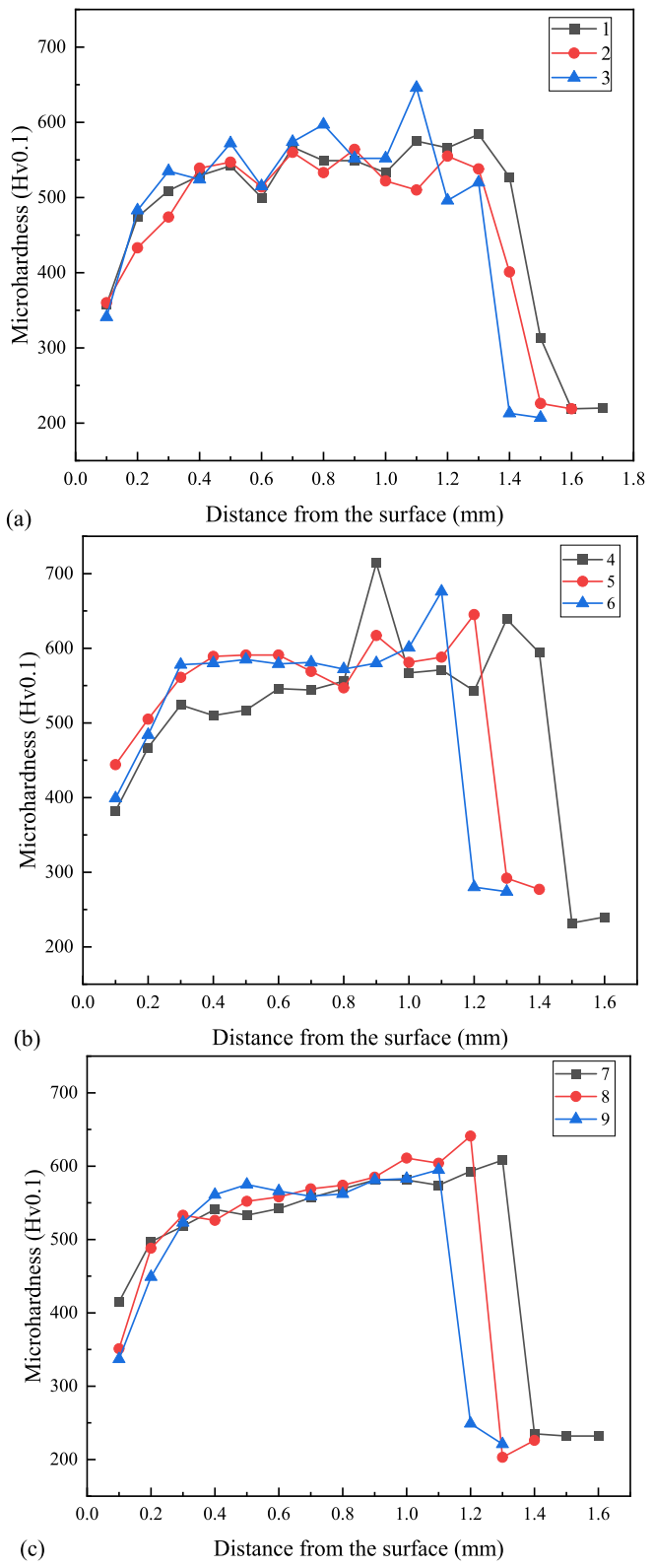

Fig. 8. Microhardness profiles as functions of the distance from the surface for different samples. The samples were cut from cladded ball valves with different diameters of (a) 80 mm, (b) 120 mm, and (c) 200 mm (labelled from 1 to 9).

valve, which can fuse the powder to a thinner cladding layer. On the other hand, for the same scanning speed, the cladding height also shows a downtrend as ball valve increases in diameter. The larger the diameter of the ball valve, the less surface curvature will be. This means that larger diameter ball valves are easier to wrap and process with the rectangular beam. However, higher thermal conduction capability of the ball valves with large diameter results in a part of the laser energy being transferred to the surrounding substrate. Because of that, the temperature of molten pool decreases, and the efficiency of powder catchment descends.

As explained before, the smaller the ball valves, the more demanding the cladding technology eliminating cracks will be. Therefore, the cut sample from the ball valve with 80 mm is adopted for microscopic testing. Fig. 6 shows a cross-sectional micrograph of the cladded sample. As can be seen, the powder is melted to form a dense cladding coating on the substrate. It is worth noting that the WC particles remain more in the initial phase and are well embedded in the Ni-based substrate, which can be attributed to higher melting point of the WC particles than that of Ni-based power. Furthermore, the WC particles are mainly distributed in the lower part of the cladding layer, and only a few smaller particles are present in the middle and upper parts. This is probably due to the fact that the density of the WC particles is higher than that of the Ni-based powder.

In order to check the microstructure particularly, SEM images at the interface of the cladding layer and substrate using scanning electron microscope (SEM, JEOL JSM-7900F) are shown in Fig. 7. There are two colors in images, the upper part is the cladding layer material, the lower is the substrate. It can be found that the interface is well bound and the cladding layer is almost free from cracks and pores. It can be attributed to two main reasons. On one hand, a pre-set powder feeding method is employed in the experiment. In this way, the ball valve to be processed is rotated by the CNC table, while the laser processing head and powder nozzle fixed on the 6-axis robotic arm are kept in a fixed position with respect to the ball valve, so that the cladding powder can be ejected uniformly on the ball valve and keep a constant shape. On the other hand, the traditional laser source usually yields a very small beam spot with a high-power density, causing narrow cladded stripes in the laser cladding; hence, it is necessary to have multiple passes on the ball valve. Such high-power density can remelt previous cladded stripes and be more likely to cause cracks and pores. In our case, through the beam conversion, the rectangular beam spot with a uniform power distribution is realized. The uniform energy distribution can provide a smooth cycle of heating and cooling during the cladding processing, which effectively eliminates cracks and pores in the coating.

The microhardness across the cross section of the cladded samples is measured by a Vickers-1000 tester, with 10-s dwell time and under load of $HV_{0.1}$. Fig. 8 shows the microhardness profiles for sample 1 to 9 that are measured at multiple distances from the sample surface with an increment of 0.1 nm. From the microhardness measurement results, it can be seen that the cross section of the cladding samples can be distinguished into three regions – the cladding layer, the bonding layer, and the substrate. Consistent to the microhardness tests, the microhardness of the cladding layer exhibits much higher value than that in the substrate. There is a slight increase from 500 $HV_{0.1}$ to 600 $HV_{0.1}$ within 1-mm thickness from the top surface of cladding layer. There exist several hardness values exceeding 650 $HV_{0.1}$ near the substrate, which may be due to WC particles deposited at high density. The WC particles microhardness is high, which has a strengthening effect on the cladding layer. The hardness of the bonding layer that is between the cladding layer and the substrate decreases rapidly. In addition, the hardness of the substrate remains around 210 $HV_{0.1}$, which is comparable to the standard hardness of stainless steel, indicating that the thermal effect of laser cladding does not cause a hardness drop in the substrate. Meanwhile, we observed the microstructure of samples. The sample with the size of 10 × 10 mm^2 was corroded with aqua regia. Microstructure images by Zeiss metallographic optical microscope (Axioscope 5) are shown in Fig. 9. The figure shows that the fusion cladding layer is dominated by columnar crystals, and the grain size in the junction zone is larger than that in the middle than in the upper part. This may be due to the layer-by-layer cladding, the upper layer heat

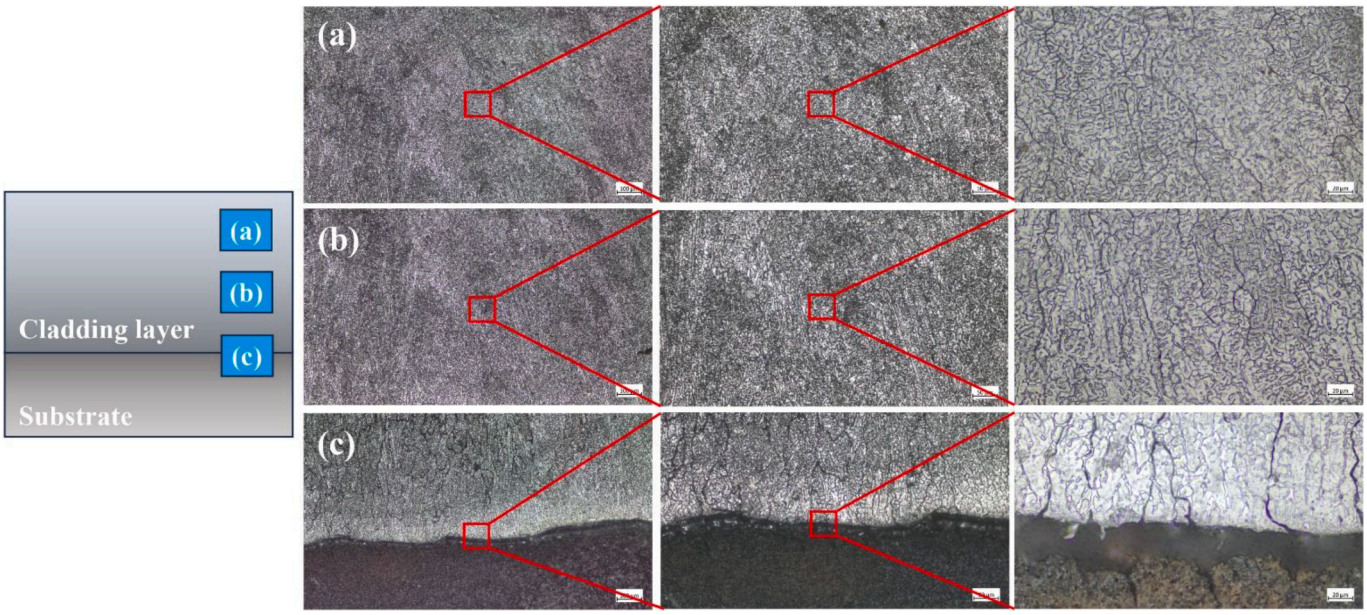

Fig. 9. Microstructure images by Zeiss metallographic optical microscope (Axioscope 5). Regions of interest are magnified from left to right.

source will have a remelting effect on the lower layer, creating a heat-affected zone and causing grain regrowth.

4. Conclusion

In this paper, in order to reduce the overlapping frequency and eliminate cracks of the laser cladding layer on the stainless-steel ball valves, a novel diode laser source based on the rectangular bean spot with the effective dimension of 16 × 1 mm^2 was proposed and demonstrated for laser cladding. Using this diode laser source, the laser cladding of the stainless-steel ball valve is successfully completed with the Ni60 + WC powder. The highest microhardness of the cladding layer is 600 $HV_{0.1}$, which meets the demands of most industrial applications. In comparison to the traditional circular beam spot with a Gaussian distribution, the rectangular beam spot with a flat-top distribution has the advantages of large processing area and little temperature gradient, which makes its cladding effect better. This work not only provides a new method for laser cladding of stainless-steel ball valves, but paves the way for the future research of diode laser processing. Due to the low power density of rectangular beam spot, the maximum output power of the diode laser source used in the experiment, i.e., 2 kW, is the current achievable laser power for the minimum requirement of laser cladding. Therefore, the study about the influence of laser power on cladding quality has not been conducted. This work will be carried out in the future.

Funding

This work was supported by the National Natural Science Foundation of China (62222410, 62205336) and Projects of Jilin Province Science and Technology Development Plan (20210201019GX, 20220201090GX).

Declaration of Competing Interest

The authors declare that they have no known competing financial interests or personal relationships that could have appeared to influence the work reported in this paper.

Data availability

No data was used for the research described in the article.

References

[1] F. Arias-González, J. del Val, R. Comesaña, J. Penide, F. Lusquiños, F. Quintero, A. Riveiro, M. Boutinguiza, J. Pou, Fiber laser cladding of nickel-based alloy on cast iron, Appl. Surf. Sci. 374 (2016) 197–205.
[2] H. Liu, X. Qin, S. Huang, Z. Hu, M. Ni, Geometry modeling of single track cladding deposited by high power diode laser with rectangular beam spot, Opt. Lasers Eng. 100 (2018) 38–46.
[3] M. Gao, S. Li, W. Guan, H. Xie, X. Wang, J. Liu, H. Wang, Excellent thermal shock resistance of NiCrAlY coatings on copper substrate via laser cladding, J. Mater. Sci. Technol. 130 (2022) 93–102.
[4] J. Liu, H. Yu, C. Chen, F. Weng, J. Dai, Research and development status of laser cladding on magnesium alloys: A review, Opt. Lasers Eng. 93 (2017) 195–210.
[5] L. Zhu, P. Xue, Q. Lan, G. Meng, Y. Ren, Z. Yang, P. Xu, Z. Liu, Recent research and development status of laser cladding: A review, Opt. Laser Technol. 138 (2021) 106915.
[6] W. Yuan, R. Li, Z. Chen, J. Gu, Y. Tian, A comparative study on microstructure and properties of traditional laser cladding and high-speed laser cladding of Ni45 alloy coatings, Surf. Coat. Technol. 405 (2021) 126582.
[7] A.A. Siddiqui, A.K. Dubey, Recent trends in laser cladding and surface alloying, Opt. Laser Technol. 134 (2021) 106619.
[8] Z. Li, O. Allegre, L. Li, Realising high aspect ratio 10 nm feature size in laser materials processing in air at 800 nm wavelength in the far-field by creating a high purity longitudinal light field at focus, Light Sci. Appl. 11 (1) (2022) 339.
[9] P.S. Salter, M.J. Booth, Adaptive optics in laser processing, Light Sci. Appl. 8 (6) (2019) 950–965.
[10] Y. Lin, C. Jiang, Z. Lin, Q. Chen, Y. Lei, H. Fu, Laser in-situ synthesis of high aspect ratio TiB fiber bundle reinforced titanium matrix composite coating, Opt. Laser Technol. 115 (2019) 364–373.
[11] H. Yan, P. Zhang, Q. Gao, Y. Qin, R. Li, Laser cladding Ni-based alloy/nano-Ni encapsulated h-BN self-lubricating composite coatings, Surf. Coat. Technol. 332 (2017) 422–427.
[12] Y. Ding, R. Liu, J. Yao, Q. Zhang, L. Wang, Stellite alloy mixture hardfacing via laser cladding for control valve seat sealing surfaces, Surf. Coat. Technol. 329 (2017) 97–108.
[13] Z. Zhang, P. Farahmand, R. Kovacevic, Laser cladding of 420 stainless steel with molybdenum on mild steel A36 by a high power direct diode laser, Mater. Des. 109 (2016) 686–699.
[14] M. Song, L. Wu, J. Liu, Y. Hu, Effects of laser cladding on crack resistance improvement for aluminum alloy used in aircraft skin, Opt. Laser Technol. 133 (2021) 106531.
[15] Q. Chai, Z. Wang, C. Fang, Y. Xing, X. Qiu, Z. Zhou, Numerical and experimental study on the profile of metal alloys formed on the inclined substrate by laser cladding, Surf. Coat. Technol. 422 (2021) 127494.
[16] N. Sommer, F. Stredak, S. Böhm, High-Speed Laser Cladding on Thin-Sheet-Substrates—Influence of Process Parameters on Clad Geometry and Dilution, Coatings (2021).

[17] Z. Lin, H. Yu, T. Yu, Z. Zhu, Numerical study of solid–liquid two-phase flow and erosion in ball valves with different openings, Adv. Powder Technol. 33 (5) (2022) 103542.
[18] X. Lin, P. Wang, H. Zhu, Z. Song, Y. Zhang, Y. Ning, A novel processing method based on the 3-spot diode laser source for the laser cladding of stainless-steel ball valves, Opt. Laser Technol. 141 (2021) 107142.
[19] J. Malchus, V. Krausea, A. Koestersa, D.G. Matthews, A 25kW fiber-coupled diode laser for pumping applications, Proc. SPIE 8965 (2014) 89650B.
[20] F. Kubacki, H. Weitze, P. Bruns, T. Lu, Successful diode laser material processing using application specific micro-optical beam shaping, Proc. SPIE 6824 (2007) 682403.
[21] H. Zhu, X. Lin, Y. Zhang, J. Zhang, B. Wang, J. Zhang, L. Qin, Y. Ning, H. Wu, kW-class fiber-coupled diode laser source based on dense spectral multiplexing of an ultra-narrow channel spacing, Opt. Express 26 (19) (2018) 24723–24733.